Study of Aggregates of Fullerene-Based Ionomers in Aqueous Solutions Using Small Angle Neutron and X-ray Scattering

U-Ser Jeng, Tsang-Lang Lin,* Cheng-Si Tsao, and Chih-Hao Lee

Department of Engineering and System Science, National Tsing Hua University, Hsinchu 30043, Taiwan

Taizoon Canteenwala, Lee Y. Wang, and Long Y. Chiang

Center for Condensed Matter Sciences, National Taiwan University, Taipei 10617, Taiwan

Charles C. Han

Polymer Division, National Institute of Standards and Technology, Gaithersburg, Maryland 02899

Received: August 24, 1998; In Final Form: November 30, 1998

Water solutions of starlike hexaanionic fullerene derivatives, $C_{60}[(CH_2)_4SO_3Na]_6$ (star-ionomer) consisting of a C_{60} cage covalently bonded with six ionic sulfonate arms, were studied using small-angle neutron scattering (SANS) and small-angle X-ray scattering (SAXS). Nearly monodisperse aggregates of the novel star-ionomers were observed in the solutions of concentrations from 4% down to 0.5%. The structure of the spherical-like aggregates bears high similarity in different concentrations studied. Information regarding the aggregation number, hydration number, size, and shape of the aggregates was obtained from a combined analysis of the SANS and SAXS data.

Introduction

The scope of the science and technology of C_{60} (fullerene) has been broadened recently by the development of fullerene derivatives containing polar functions, such as hydroxy and/or amino groups. For instance, the water-compatible polyhydroxylated C_{60} (fullerenol) consisting of a C_{60} cage covalently bonded with hydroxy functional groups (OH) is a versatile intermediate in synthesizing hypercross-linked[1] or dendritic polymers.[2] One application of fullerenols is the synthesis of fullerenol hypercross-linked poly(urethane-ether) elastomers, which have been shown to exhibit greatly enhanced properties over the conventional polyurethane elastomers.[3] Another direction of the application for fullerenols involves the synthesis toward amphiphilic C_{60} derivatives.[4,5] In our research group Canteenwala et al. have synthesized a starlike fullerene derivative $C_{60}[(CH_2)_n$-$SO_3Na]_6$ containing an average of six ionic sulfonate arms. With the C_{60} cage and the CH_2 (alkyl) chains forming a hydrophobic core and the ionic sulfonate end groups as hydrophilic components, this novel starlike molecule has the amphiphilic property resembling that of molecular micelles, exhibiting high solubility in water. In practice, the star-ionomers comprised of extended alkyl arms may be expected to hold lipid molecules in water better than a complex system of an oil-in-water microemulsion which often dissociates due to a variation of temperature or concentration.[6,7] This aspect of molecular architecture engineering should lead to the implication of potential biomedical applications.

Using SANS and SAXS we focus the present study on the structures and the aggregation behaviors of a star-ionomer, C_{60}-$[(CH_2)_nSO_3Na]_6$ with $n = 4$, in water solutions. The extended three-component (oil/water/star-ionomer) system, although also intriguing, will be deferred to a later study.

* Author to whom correspondence should be addressed. Fax: 886-3-5728445; E-mail: tllin@ne.nthu.edu.tw.

The use of small-angle scattering (SAS) in the studies of colloidal solutions[8,9] is fruitful considering, especially in the case of SANS, its unique possibility of contrast variation by selective H/D substitution (deuteration). With this merit, Wignall et al.[10] have studied the size and shape of the polymer-grafted fullerenes in a deuterated solvent using SANS. In determining an ionic micellar structure, Liu et al.[11] and Zemb et al.[12] have also demonstrated the advantage of utilizing a combined analysis of SANS and SAXS measurements for macroion solutions. The intrinsically different cross-sections of a scattering system for neutrons and X-rays can provide contrast and/or complemental structural information for the system studied. This is particularly useful in studying fullerene-based derivatives, since the scattering-length-density (SLD) of a fullerene cage is high for both neutrons and X-rays.

Scattering Basics for Colloidal Solutions. For a colloidal solution of monodispersity the small-angle scattering cross-section per unit volume can be written as

$$I(Q) = n_p P(Q) S(Q) \tag{1}$$

where $Q = (4\pi/\lambda)\sin(\theta/2)$ is the scattering vector defined by the scattering angle θ and the wavelength λ of the radiation. We denote n_p as the number density of particles in the solution, $P(Q) = |F(Q)|^2$ the intraparticle structure factor (form factor), and $S(Q)$ the interparticle structure factor.[8] For a homogeneous spherical particle with a radius R, the particle form factor $F(Q) = (4/3)\pi R^3(\rho - \rho_s)(3j_1(QR)/QR)$ where ρ and ρ_s are the SLD for the particle and the solvent, respectively, and j_1 is the first-order spherical Bessel function.[9]

In a suspension of weak interaction or a dilute solution where $S(Q) \sim 1$, the scattering intensity in (1) is significantly simplified, and the size information can be revealed from the radius of gyration R_g obtained using the Guinier approximation[13]

10.1021/jp9834659 CCC: $18.00
Published on Web 01/30/1999

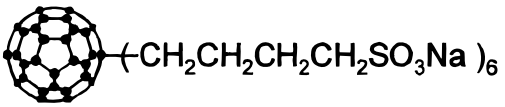

Figure 1. Schematic drawing of a star-ionomer

in the small Q region ($QR < 1$) where

$$I(Q) = I(0)\exp(-Q^2R_g^2/3) \quad (2)$$

The coefficient in eq 2 can be expressed as

$$I(0) = n_p|b_{tot} - V_p\rho_s|^2 \quad (3)$$

where b_{tot} is the total scattering length of the particle for neutrons or X-ray, and V_p refers to the solvent-excluded volume (dry volume)[9] of the particle. For a spherical and homogeneous particle $V_p = (4/3)\pi R^3$ where $R = (5/3)^{1/2}R_g$.

Experiment and Analysis

Synthetic Description. The sodium salt of hexa(sulfobutyl)-fullerenes, $C_{60}(CH_2CH_2CH_2CH_2SO_3Na)_6$ (Figure 1), were synthesized in a yield of 80−85% by the treatment of fullerene molecules in a mixture of toluene and tetrahydrofuran or dimethoxyethane (DME) with sodium naphthalide (10.0 equiv.) in DME at ambient temperatures, followed by reacting of the resulting hexaanionic fullerene intermediates with an excess of 1,4-butane sultone. The reaction was carried out under N_2 in a glovebox which was conditioned to under 50 ppm of O_2 to minimize the partial oxidation of fullerenic anions by dissolved O_2. Electron oxidation of anionic C_{60} intermediates by O_2 may produce the corresponding fullerenic radicals. A highly conjugated radical of a multi-sulfobutylated fullerene derivative was found to be rather stable at ambient temperatures. Its electron spin resonance (esr) was readily detectable in the aqueous solution. Even under rigorously deoxygenated conditions, the persistence of fullerenic radicals in the resulting products was evident from repeated reactions. Therefore, an excess of sodium naphthalide was found to be necessary to achieve the generation of hexaanionic fullerene intermediates. The product was purified by a chromatographic method to exhibit a single peak in its HPLC profile using a reverse-phase C-18 column with water as eluant. Infrared spectra of hexa(sulfobutyl)fullerenes displayed a broad absorption band centered at 3444 cm^{-1} (owing to a hydrated molecule) along with two strong absorptions centered at 1178 cm^{-1} and 1050 cm^{-1}, corresponding to the stretching bands of the sulfonic acid salt with a $C-SO_2-O$ linkage. The mass spectroscopic studies were carried out using the matrix-assisted laser desorption ionization (MALDI) techniques. The negative ion MALDI mass spectrum of hexa-(sulfobutyl)fullerene showed a conceivable molecular ion of $C_{60}(CH_2CH_2CH_2CH_2SO_3H]_6$ at m/z 1542. It was followed by two groups of ion fragmentations with a maximum intensity of peak at m/z 1405 and 1269 corresponding to the mass of $C_{60}(CH_2CH_2CH_2CH_2SO_3H]_5$ and $C_{60}(CH_2CH_2CH_2CH_2SO_3H]_4$, respectively. These mass spectroscopic data provided a clear evidence of the chemical composition for the hexa(sulfobutylated)fullerene compound.

SAS Measurements. For SANS measurements, D_2O was selected for its much lower incoherent scattering background as compared with H_2O.[8] Two sample solutions with a concentration of 1 wt % and 4 wt % in D_2O were separately charged in quartz cells of 5 mm in path length. The SANS measurements were conducted at a sample temperature of 25 °C on the 8 m SANS instrument at the National Institute of Standards and Technology (NIST). Pinholes of 2.5 cm and 1 cm diameters separated by 4.1 m were used to collimate the incident beam which has a wavelength dispersion $(\Delta\lambda/\lambda)_{fwhm} = 25\%$. Equipped with a beam wavelength of 5 Å and a sample-to-detector distance of 3.6 m, the SANS instrument covered a Q range from 0.02 $Å^{-1}$ to 0.2 $Å^{-1}$. The sample transmissions, $T = 0.66$, measured for these two concentrations were nearly identical within a 5% accuracy. Data were corrected for sample transmission, background, and detector sensitivity, and normalized to the scattering cross section per unit sample volume (the absolute intensity).

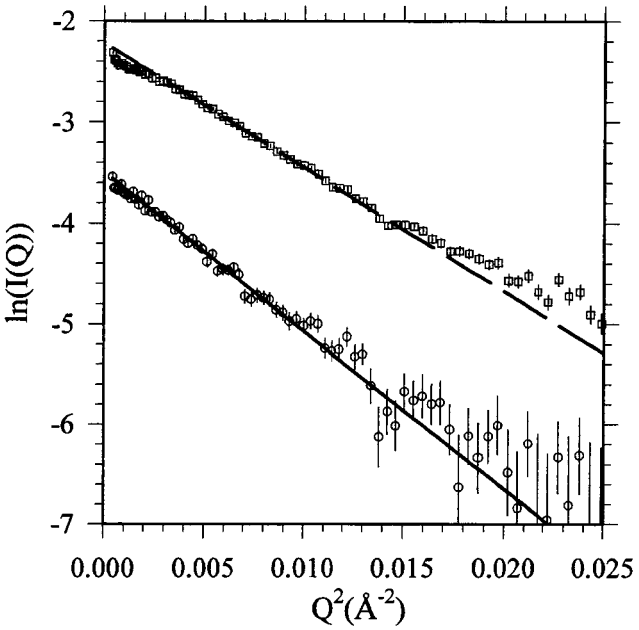

Figure 2. Guinier plots for the SANS data of the $C_{60}[(CH_2)_4SO_3Na]_6$ solutions of 1 wt % (circles) and 4 wt % (squares) in D_2O. The R_g values obtained from the Guinier approximations are 21.7 Å (solid line) for 1 wt % and 19.2 Å (dashed line) for 4 wt % data.

For SAXS measurements, sample solutions with a concentration of 0.5, 1.0, 2.0, and 4.0 wt % in H_2O were transferred individually into sample cells of 1 mm path length nominally. The thickness for each Kapton window of the sample cell was 25 μm.

The SAXS measurements were performed at a sample temperature of 25 °C on the 8-m SAXS instrument at Tsing-Hua University, Hsinchu.[14] This instrument was equipped with an 18 kW rotating-anode X-ray source and a copper target. The beam collimation system consisted of three pinholes (1.5 mm, 1.2 mm, and 2.0 mm in diameter, respectively) arranged in 3.1 m path length. With the beam wavelength of 1.54 Å monochromated by a pyrolytic graphite and a sample-to-detector distance of 4.1 m, the SAXS instrument scanned the scattering intensity in a Q range from 0.01 $Å^{-1}$ to 0.12 $Å^{-1}$. Data were collected by a two-dimensional area detector, and normalized to the absolute intensity using the same procedure as that applied for the SANS data.

SANS Results. Figure 2 shows the SANS data collected for the sample solutions containing 1 wt % (circles) and 4 wt % (squares) star-ionomers. The scattering profiles for these two samples bear a close resemblance to each other, indicating a high similarity in structures of the scattering particles in these solutions. Each set of the data follows, respectively, the Guinier approximation for the 1% (solid line) and 4% data (dotted line) closely up to large Q values ($QR \sim 4$), which suggests that the scattering intensity is contributed by nearly isodiametric ag-

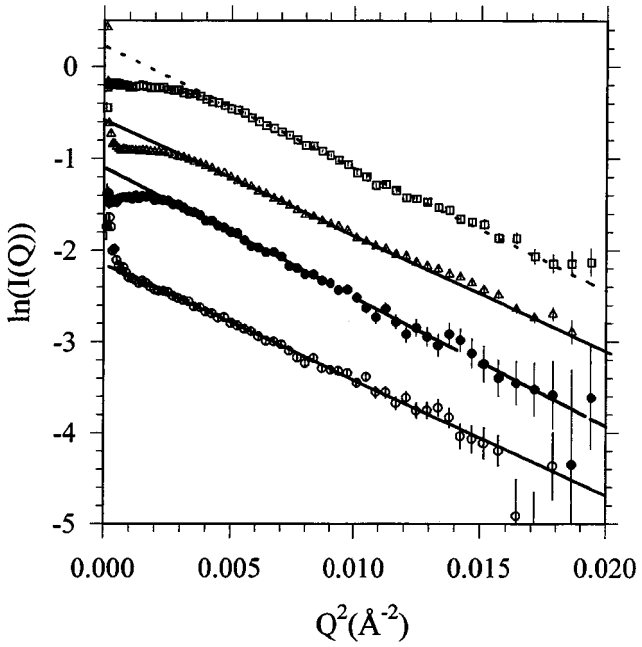

Figure 3. SAXS data for the sample solutions of 0.5 wt % (open circles), 1 wt % (solid circles), 2 wt % (triangles), and 4 wt % (squares) of $C_{60}[(CH_2)_4SO_3Na]_6$ in H_2O are fitted, respectively, using the Guinier approximation of R_g values of 19.5, 20.6, 19.5, and 20.0 Å (solid, long-dashed, short-dashed, and dotted lines).

gregates of star-ionomers.[13] The R_g values obtained by the Guinier approximation are 21.7 ± 1.8 Å for the 1% data and 19.2 ± 0.2 Å for the 4% data. The mean radius of the small aggregates, $R = (5/3)^{1/2}R_g$, deduced from 1% data is about 28 Å. This radius is much larger than the estimated size of a single star-ionomer molecule with fully stretched arms ($R \sim 15$ Å),[11,15] which is clear evidence of the existence of small aggregates. The profile of the 4% data deviates slightly from the Guinier approximation in the lower Q region, implying weak interactions among the aggregates.[8]

We also investigated the polydispersity, p, of the small aggregates using a Gaussian size distribution of spheres[16] as well as the indirect transform method.[17] Both results show a small percentage ($p \sim 10\%$) of polydispersity for the 4% data, and a vanishing p for the 1% data. This result is consistent with the conclusion of nearly monodisperse aggregates obtained previously.

In addition, models of disklike and/or rodlike structures for the aggregates are also examined using the Kratky−Porod approximation.[18] The results show both models being inappropriate.

SAXS Results. Figure 3 shows the SAXS data measured at 25 °C for the sample solutions containing 0.5 wt % (open circles), 1 wt % (solid circles), 2 wt % (triangles), and 4 wt % (squares) of $C_{60}[(CH_2)_4SO_3Na]_6$ in H_2O. Besides the scattering peaks in the very low Q ($\lesssim 0.015$ Å^{-1}) region due to the instrumental resolution, the scattering profiles for these four concentrations are essentially close in shape to each other, suggesting the formation of similar packing structures of star-ionomer aggregates in these concentrations. The data for 0.5%, 1%, 2%, and 4% sample solutions can all be fitted well up to large Q values using the Guinier approximation with R_g values of 19.5 ± 0.2 Å (solid line), 20.6 ± 0.2 Å (long dashed line), 19.5 ± 0.2 Å (short dashed line), and 20.0 ± 0.3 Å (dotted lines), respectively.

In the lower Q region of Figure 3 the deviations of data from the Guinier approximations are due to the interparticle interactions between the aggregates. The degree of deviation decreases as the concentration decreases and reaches a vanishing level as shown in the 0.5% data. Therefore, the form factor of the aggregates for a 0.5% solution can be determined from the scattering profile unequivocally since $S(Q) \approx 1$. A well-determined form factor is useful in extracting interparticle structure factors for the solutions of higher concentrations. The effect of interparticle interactions is more pronounced and can be clearly observed in the SAXS data, because the SAXS has a much higher Q-resolution than that for the SANS. Note the much higher scattering intensity of SAXS (~10-fold) than that of SANS measured under the same concentration.

TABLE 1: Summary of the SANS and SAXS Results[a]

	C (wt %)	$I(0)$ (cm^{-1})	R_g (Å)
SANS (in D_2O)	1	0.030 ± 0.001	21.7 ± 1.8
	4	0.109 ± 0.002	19.2 ± 0.2
SAXS (in H_2O)	0.5	0.116 ± 0.001	19.5 ± 0.2
	1	0.334 ± 0.003	20.6 ± 0.2
	2	0.561 ± 0.005	19.5 ± 0.2
	4	1.256 ± 0.025	20.0 ± 0.3

[a] The notation C is for the sample concentration, and $I(0)$ for the scattering intensity at $Q = 0$ (from the Guinier approximation). R_g is the radius of gyration for the small aggregates of star-ionomers.

Comparative SAXS measurements were also performed on both solutions of D_2O and H_2O containing 1% by wt of sample. The SAXS data from these two solutions are nearly identical after the normalization by molar concentration. This indicated the lack of isotope effect during the forming of the aggregates.[12] To evaluate the potential temperature effect on the aggregation of ionomers, we measured a 2 wt % sample solution at 8, 25, and 50 °C, and found no obvious change in the scattering profile at these temperatures.

Structure of the Aggregate. Aggregation features of the star-ionomers derived from the SAXS data agree well with that concluded from the SANS results (see Table 1). In fact, by ignoring the low-Q (<0.02 Å^{-1}) data, the scaled SAXS profiles for the 4% and 1% sample solutions can superimpose well with the corresponding SANS data, especially in the case of 1% data (Figure 4). This indicates the form factor of the small aggregates for SAXS is very similar to that for SANS, since $S(Q)$ is the same for both SANS and SAXS. Therefore, we use the SANS and SAXS data as a contrast to determine the structure of the aggregate as shown below.[16,19] Our method differs from others[11,12] where SANS and SAXS data collected for the same system were used complementarily to elucidate the structure of an ionic micelle.

From eq 3 the zero-Q intensity $I_N(0)$ and $I_X(0)$ respectively for SANS and SAXS can be expressed as

$$I_N(0) = NC|b_{c,N} - V_c\rho_{s,N}|^2 \quad (4)$$

and

$$I_X(0) = NC|b_{c,X} - V_c\rho_{s,X}|^2 \quad (5)$$

where N is the mean number of star-ionomers for the aggregate and C is the number of star-ionomers per unit sample volume, with $C = Nn_p$. We denote $b_{c,N}$ ($b_{c,X}$) and $\rho_{s,N}$ ($\rho_{s,X}$), individually, as the scattering length of the star-ionomer and the SLD of the solvent for neutrons (X-ray), whereas V_c is the dry volume for the star-ionomer. Using eqs 4 and 5, and the numerical values $I_N(0) = 0.030$ cm^{-1} and $I_X(0) = 0.334$ cm^{-1} (see Table 1) extrapolated from the 1% SANS (in D_2O) and SAXS (in H_2O)

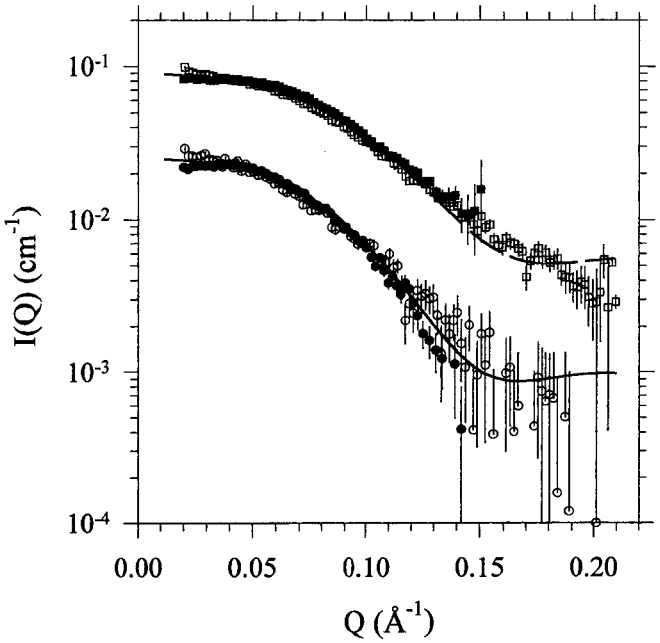

Figure 4. The comparison of the SANS and SAXS data. The 4% (closed squares) and 1% (closed circles) SAXS data are scaled down by a factor 10 to the corresponding 4% (open squares) and 1% (open circles) SANS data. The SANS and SAXS data are fitted simultaneously (solid and dashed curves for 1% and 4% data, respectively) using a simple model of monodisperse spheres with a hard-sphere potential. Note data in the $Q < 0.02$ Å^{-1} region are not shown.

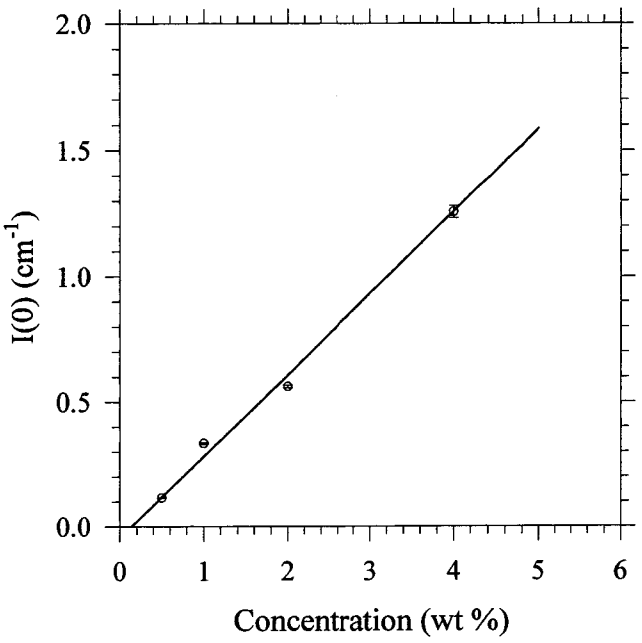

Figure 5. $I(0)$ extrapolated from the Guinier approximation for the SAXS data versus the sample concentration. These $I(0)$ values fall on a straight line which intercepts $I(0) = 0$ at 0.13 wt %. This gives an estimation of a threshold concentration for forming aggregates of star-ionomers.

data by using Guinier approximation, and $b_{c,N} = 5.225 \times 10^{-3}$ Å, $b_{c,X} = 2.420 \times 10^{-2}$ Å, $\rho_{s,N} = 6.36 \times 10^{-6}$ Å^{-2}, and $\rho_{s,X} = 9.44 \times 10^{-6}$ Å^{-2}, we solve the two parameters $N = 7.0 \pm 0.9$ and $V_c = 1340 \pm 20$ Å^3. The value of V_c obtained is consistent with an estimated value of 1600 Å^3 from the volume of C_{60} cage[15] with 6 sulfobutyl chains.[11] Using the volume of the aggregate $V_a = NV_c + MV_w$ where $V_w = 30$ Å^3 is the volume of a water molecule,[11] and M is the number of water molecules in each aggregate (hydration number), we deduce $M = 2500 \pm 450$. The value for V_a is estimated from a spherical particle with a radius of 27.2 Å given by the averaged R_g value derived from the SANS and SAXS data of the 1% sample solution. This result indicates an association of 60 water molecules, on average, on each sulfonate headgroup (SO_3Na) of the star-ionomer having six hydrophilic arms in the aqueous aggregate.

Using the same method for the 4% SANS and SAXS data as was used in the analysis of the 1% data, we obtain $N = 6.5 \pm 0.7$, $V_c = 1330 \pm 95$ Å^3, and $M = 1950 \pm 350$ for the aggregates in the 4% sample solution. These values indicate that the structure of the aggregates for the 4% solution is essentially the same as that for the 1% solution, except a smaller water content.

With $I(0)$ (from the Guinier approximation) for the SAXS data plotted as a function of concentration, as shown in Figure 5, we found all these $I(0)$ values fall on a straight line which intercepts the zero scattering intensity at a concentration of 0.13 $\pm$ 0.09 wt %. It verifies the approximation used in the above calculation for N and V_c that almost all the star-ionomers in the solution exist as a form of small aggregates.

Using a simple model of monodisperse spheres with a hard-sphere potential, we fit (solid and dashed curves in Figure 4) the SANS and SAXS data simultaneously.[11,12] The result, which will be presented elsewhere,[20] improves slightly the values (aggregation number, hydration number, size, and dry volume) given above, and does not change much the picture outlined here for the aggregates.

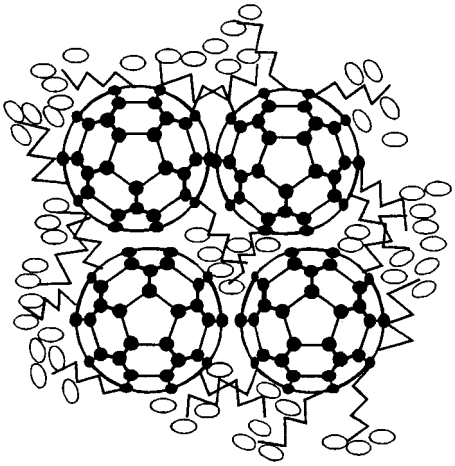

Figure 6. Schematic cross-section of an aggregate of C_{60}-derived star-ionomers in a water solution.

Discussion and Conclusions

The repulsive electrostatic potential is often used to account for the strong interference between ionic micelles in a macroion solution, e.g., a sodium dodecyl sulfate (SDS) solution.[21] The interparticle interaction between the aggregates of star-ionomers we observed, however, is much weaker and insensitive to the temperature change for the concentrations studied. These are the characteristics for the interaction of a hard-sphere-like potential.[22] Such an interaction behavior may result from the watery structure of the star-ionomer aggregate which has a homogeneous charge distribution rather than the two-shell distribution for an ionic micelle.[11,12] As a consequence, its net-surface-charge-density $\sigma_s \approx 4 \times 10^{-4}$ e$^-$/Å^2 is much lower than, for instance, $\sigma_s \approx 2 \times 10^{-3}$ e$^-$/Å^2 for the ionic micelle of SDS.[12,21] Here, we have used 0.2 as an ionization factor for the sulfate groups.[11]

The driving force for the aggregation of star-ionomers should be due to their hydrophobicity. It is possible that the sulfobutyl chains are not symmetrically anchored on the fullerene cage. This results in exposing a larger hydrophobic area on the surface of the fullerene cage which leads to an aggregation for minimizing the free energy of the system. The intermolecular interaction between the hydrophobic butyl arms anchored on neighboring star-ionomers may also contribute to the aggregation of the C_{60}-derived star-ionomers. A schematic picture proposed for the aggregate is shown in Figure 6.

We have studied the aggregation behaviors of star-ionomers in water solutions using SANS and SAXS. The nearly monodisperse aggregates have a spherical-like structure with a relatively homogeneous SLD for SANS as well as for SAXS. The size of the aggregate is about the same for all concentrations studied. The interaction between the aggregates is weak and insensitive to the temperature change. The aggregation and hydration number for the watery aggregates are determined from the SANS and SAXS data.

Acknowledgment. We thank Dr. M. Y. Lin and Dr. L.-P. Sung of the Reactor Radiation Division at NIST, and W.-J. Liu of the Department of Engineering and System Science at National Tsing Hua University for experimental assistance. We acknowledge the support of the National Institute of Standards and Technology for the use of the 8 m SANS. This work was supported by the travel grant for the user training program of the Institute of Nuclear Energy Research, and the National Science Council, grant NSC87-2113-M-007-010 (T.-L. Lin) and grant NCS87-2216-E002-021 (L.Y. Chiang).

References and Notes

(1) Wang, L. Y.; Wu, J.-S.; Tseng, S.-M.; Kuo, C.-S.; Hsieh, K.-H.; Liau, W.-B.; Chiang, L. Y. *J. Polym. Res.* **1996**, *3*, 1; Chiang, L. Y.; Wang, L. Y.; Kuo, C. S. *Macromolecules* **1995**, *28*, 7574.

(2) Chiang, L. Y.; Wang, L. Y.; Tseng, S. M.; Wu, J. S.; Hsieh, K. H. J. *Chem. Soc., Chem. Commun.* **1994**, 2675.

(3) Chiang, L. Y.; Wang, L. Y. *Trends in Polym. Sci.* **1996**, *4*, 298.

(4) Vaknin, D. *Physica B* **1996**, *221*, 152.

(5) Matsumoto, M.; Tachibana, H.; Azumi, R.; Tanaka, M.; Nakamura, T.; Yunome, G.; Abe, M.; Yamago, S.; Nakamura, E. *Langmuir* **1995**, *11*, 660.

(6) Meunier, J. *J. Phys. Lett.* **1985**, *46*, L-1005.

(7) Langevin, D. *Light Scattering by Liquid Surfaces and Complementary Techniques*; Langevin, D., Ed.; Marcel Dekker: New York, 1992; Chapter 13.

(8) Chen, S. H.; Lin, T. L. *Methods of Experimental Physics − Neutron Scattering in Condensed Matter Research*; Sköld, K., Price, D. L., Eds.; Academic Press: New York, 1987; Vol. 23B, Chapter 16.

(9) Chen, S.-H. *Annu. Rev. Phys. Chem.* **1986**, *37*, 351.

(10) Wignall, G. D.; Affholter, K. A.; Bunick, G. J.; Menceloglu, Y. Z.; Desimone, J. M.; Samulsi, E. T. *Macromolecules* **1995**, *28*, 6000.

(11) Liu, Y. C.; Ku, C. Y.; LoNostro, P.; Chen, S.-H. *Phys. Rev. E* **1995**, *51*, 4598.

(12) Zemb, T.; Charpin, P. *J. Phys. (Paris)* **1985**, *46*, 249.

(13) Guinier, A.; Fournet G. *Small-Angle Scattering of X-rays*; John Wiley and Sons: New York, 1955.

(14) Linliu, K.; Chen, S.-A.; Yu, T. L.; Lin, T.-L.; Lee, C.-H.; Kai, J.-J.; Chang, S.-L.; Lin, J. S. *J. Polym. Res.* **1995**, *2*, 63.

(15) Henderson, S. J. *Langmuir*, **1997**, *13*, 6139.

(16) Bendedouch, D.; Chen, S.-H.; Koehler, W. C. *J. Phys. Chem.* **1983**, *87*, 153.

(17) Tsao, C. S.; Lin, T. L. *J. Appl. Crystallogr.* **1997**, *30*, 353.

(18) Lin, T.-L. *Physica B* **1992**, *180*, 505.

(19) Lin, T.-L.; Liu, C.-C.; Roberts, M. F.; Chen, S.-H. *J. Phys. Chem.* **1991**, *95*, 6020.

(20) Tsao, C.-S.; Lin, T.-L., and Jeng, U. To be published in *J. Phys. Chem. Solids*.

(21) Hayter, J. B.; Penfold, *J. Chem. Soc., Faraday Trans. 1*, **1981**, *77*, 1851.

(22) Reichl, L. E. *A Modern Course in Statistical Physics*; University of Texas Press: Austin, 1988; Chapter 11.